AstraNav-World: World Model for Foresight Control and Consistency

Junjun Hu[1][*][†][✉], **Jintao Chen**[1,2][*], **Haochen Bai**[1,*], **Minghua Luo**[1], **Shichao Xie**[1], **Ziyi Chen**[1], **Fei Liu**[1], **Zedong Chu**[1], **Xinda Xue**[1,2], **Botao Ren**[1,3], **Xiaolong Wu**[1], **Mu Xu**[1], **Shanghang Zhang**[2][✉]

[1]**Amap Alibaba**, [2]PKU, [3]THU
[*]Equal Contribution, [†]Project Lead., [✉]Co-corresponding authors

Embodied navigation in open, dynamic environments demands accurate foresight of how the world will evolve and how actions will unfold over time. We propose AstraNav-World, an end-to-end world model that jointly reasons about future visual states and action sequences within a unified probabilistic framework. Our framework integrates a diffusion-based video generator with a vision-language policy, enabling synchronized rollouts where predicted scenes and planned actions are updated simultaneously. Training optimizes two complementary objectives: generating action-conditioned multi-step visual predictions and deriving trajectories conditioned on those predicted visuals. This bidirectional constraint makes visual predictions executable and keeps decisions grounded in physically consistent, task-relevant futures, mitigating cumulative errors common in decoupled "envision-then-plan" pipelines. Experiments across diverse embodied navigation benchmarks show improved trajectory accuracy and higher success rates. Ablations confirm the necessity of tight vision–action coupling and unified training, with either branch removal degrading both prediction quality and policy reliability. In real-world testing, AstraNav-World demonstrated exceptional zero-shot capabilities, adapting to previously unseen scenarios without any real-world fine-tuning. These results suggest that AstraNav-World captures transferable spatial understanding and planning-relevant navigation dynamics, rather than merely overfitting to simulation-specific data distribution. Overall, by unifying foresight vision and control within a single generative model, we move closer to reliable, interpretable, and general-purpose embodied agents that operate robustly in open-ended real-world settings.

Date: December 25th, 2025

Project Page: https://astra-amap.github.io/AstraNav-World.github.io/

⭐ Astra

1 Introduction

Embodied navigation is a core capability of embodied intelligence, aiming to enable agents to act and make decisions autonomously in complex, unknown real environments Yang et al. (2025); Zhang et al. (2025a); Wang et al. (2022); Anderson et al. (2018a). Despite significant progress in perception and instruction understanding, a key reason for navigation failures remains the lack of modeling of physical laws and temporal dynamics: small prediction biases accumulate over time, ultimately undermining the effectiveness of global planning. To achieve highly reliable real-world navigation, we advocate advancing two capability pipelines in tandem—"envision the future" and "plan the future" Finn and Levine (2017); Wu et al. (2024). The former emphasizes generating credible future visual states given actions to evaluate the model's understanding of physics and causality; the latter emphasizes task-oriented action prediction, imposing constraints on visual generation so that predicted states are closer to the reachable world.

For "plan the future", a common route is to build VLA on top of a VLM by adding an action head to achieve accurate and fast trajectory prediction Nvidia et al. (2025); Wang et al. (2025). For "envision the future", a natural path is to build a world model Ali et al. (2025); Russell et al. (2025). Methods Bar et al. (2025); Zhou et al. (2025); Yao et al. (2025) like NWM follow an "imagine-then-act" paradigm: given past images and actions, it predicts future first-person frames and uses them to judge whether the action sequence is feasible. Most of these methods use a video generation model as the base model since video generation models possess strong visual priors. Additionally, to better exploit video-generation priors, some studies use large-scale video-generation pretraining to improve model generalization Lyu et al. (2025); Zitkovich et al. (2023); Cheang et al. (2024), adopting a unified latent space to represent vision, language, actions, and world states for cross-modal knowledge sharing, and training on multi-tasks (e.g., video prediction plus policy learning).

Long-horizon planning is another key challenge in embodied intelligence. VLA approaches, benefiting from strong vision-language understanding, tend to have better long-horizon planning potential; in contrast, world model-based long-horizon planning has been relatively underexplored. This has led to directions that combine the two, such as WorldVLA Cen et al. (2025) and CoT-VLA Cen et al. (2025); Zhang et al. (2025b): a single autoregressive Transformer serves both as a "world model" (generating future images) and an "action model" (generating control sequences). Among them, CoT-VLA emphasizes explicit reasoning via "intermediate visual states" to improve decision-making for complex instructions; WorldVLA points out that multi-step prediction errors can easily trigger planning collapse, requiring physical future consistency. Overall, VLAs focus on complex instructions and long-horizon planning, while world models focus on environment understanding and dynamics prediction; combining them produces complementary benefits.

However, most existing methods still follow a loosely coupled "envision-then-plan" paradigm: envisioning and planning are decoupled in the pipeline, which tends to amplify physical uncertainty and causal ambiguity, leading to inconsistencies between the two. To address this, we propose a unified generative navigation world model that tightly binds "envision the future" and "plan the future" within a single probabilistic framework. Building on a powerful VLM with long-horizon perception and instruction understanding Bai et al. (2025), we deeply couple a DiT-based video generator Wan et al. (2025) with an action policy Xue et al. (2025), jointly modeling multi-step future visual frames and action sequences conditioned on the current state and language instructions. We optimize the two complementary objectives in parallel, and they progress in lockstep via synchronized rollout. This bidirectional constraint both provides executable visual evidence to support the rationality of planning and uses policy choices to inversely constrain visual generation to stay aligned with task intent Xiu et al. (2025). As a result, we construct a long-horizon navigation architecture that is visually coherent and behaviorally effective, reducing error propagation and pipeline inconsistencies, improving robustness and success rates. Extensive experiments show that our joint framework significantly outperforms existing methods in both future trajectory prediction accuracy and overall navigation success rate. Ablation studies further validate the necessity of bidirectional coupling and joint training: removing either branch weakens the grasp of environmental physics and task constraints, causing synchronized degradation in prediction performance. This study provides three primary contributions:

- A unified generative framework in which future visual frames and action sequences are modeled simultaneously, and through bidirectional constraints and synchronized rollout under joint optimization, physical and causal consistency are reinforced, leveraging executable visual evidence to support the action, and generated frames are constrained by the action to maintain persistent alignment with task goals.

- A world-model-based navigation architecture (AstraNav-World) is proposed, where the vlm serves as a global planner and encodes the language instruction together with historical and current multi-view observations into vision–language embeddings, which are then used to condition (i) a diffusion-based video generator for state prediction and (ii) a policy head for trajectory prediction.

- Performance, interpretability, and zero-shot transfer: AstraNav-World achieves strong gains on multiple navigation benchmarks, improving SR/SPL and reducing NE compared to prior methods. Importantly, without any real-world fine-tuning, AstraNav-World demonstrates robust zero-shot transfer on a physical robot in previously unseen real environments.

In summary, we place "envision the future" and "plan the future" within a single generative model. Leveraging the long-horizon understanding of a strong VLM, we use physically consistent video generation and task-aligned policy prediction to obtain a coherent and long-horizon-appropriate navigation plan. This not only improves robustness and success in real environments but also makes decisions more interpretable and extensible.

2 Related Works

2.1 World Model

World models aim to capture environment dynamics and predict future states to support perception and decision making. Beyond short-horizon rollouts, recent work treats them as generators that synthesize future videos to provide visual evidence for planning. LaDi-WM Huang et al. (2025) employs diffusion modeling to predict future states within a geometric-semantic latent space, enabling more consistent and generalizable state forecasting compared to pixel-based approaches. MoWM Shang et al. (2025) enhances decision robustness by fusing latent and pixel predictions through feature modulation in a mixture-of-world-models architecture during planning.

In addition, world models are increasingly employed not only for prediction but as generative, interactive environments. Interactive world models condition on actions, language, or goal images to generate controllable, step-by-step futures, showcasing strong capabilities in environment simulation. Genie series Bruce et al. (2024); Parker-Holder et al. (2024) show that internet-scale video plus latent-action Transformers can yield a single, prompt-controllable world model for 2D/3D games and robotics, enabling zero-shot policy imagination without real-world rewards or labels. Yan Team (2025) enables real-time, infinite interactive video generation via cross-domain prompts using a dynamics–rendering disentanglement. World models play the same role in the navigation domain as well, are used for scene understanding and future-frame imagination to guide planning, which provides visual evidence for exploration Bar et al. (2025).

In terms of architecture, for video generation, autoregressive (AR) models and diffusion models have become the two dominant paradigms. AR world models serialize and autoregressively model multiple modalities—video, actions, and language—with representative work including MineWorld Guo et al. (2025). Their advantages include natural suitability for sequence modeling, strong scalability, and effective cross-modal fusion. Diffusion-based world models (e.g., Matrix-Game 2.0 He et al. (2025) and UWM Zhu et al. (2025a)) deliver higher generation quality, and have become the preferred choice in world generation due to their superior performance. Given our focus on generating high-fidelity, physically consistent future visual evidence for navigation and on leveraging the world understanding and physical priors from large-scale pretraining, we adopt a diffusion-based world model as our core architecture.

2.2 Combining world models with VLA

World models excel at physically consistent short-horizon rollouts for near-field planning and closed-loop control, while VLA models capture high-level semantics and generate coherent long-horizon actions. Recent work exploits this complementarity by tightly coupling the two, yielding more reliable long-horizon planning and greater interpretability.

WorldVLA Cen et al. (2025) integrates a latent world model with a VLA and produces a visual chain of thought (V-CoT) during inference to aid decision-making and enhance interpretability. DreamVLA Zhang et al. (2025b) adopts a Dreamer-style latent world model to perform "dream-like" visual rollouts and incorporates intermediate multimodal representations—such as dynamic maps, depth maps, and semantic maps into the reasoning process, providing visual evidence for multi-step planning and manipulation. CoT-VLA Zhao et al. (2025) explicitly injects visual intermediate goals into VLA by first autoregressively predicting future frames as visual subgoals and then generating short action sequences, thereby unifying temporal planning and interpretability. GigaBrain-0 Team et al. (2025) integrates RGB-D sensory modeling with embodied chain-of-thought supervision to systematically enhance reasoning over spatial geometry, object-state estimation, and long-horizon temporal dependencies. FlowVLA Zhong et al. (2025) uses Visual CoT to predict optical flow before next-frame synthesis, aligning dynamics pretraining with action generation and improving physical plausibility and sample efficiency.

Unlike the above works, we move away from the loosely coupled "envision-then-then" paradigm and instead deeply couple video generation (world modeling) and action generation (policy modeling) within a single probabilistic generative process with synchronized rollout. At each step, the two are mutually conditioned and cross-corrected, reducing cross-modal inconsistencies and long-horizon error accumulation.

3 Method

3.1 Overall Architecture

Our AstraNav-World is a unified generative world model that tightly couples future vision prediction with action prediction within a single probabilistic framework. Unlike conventional "envision-then-plan" approaches that treat these components as separate modules, our architecture ensures bidirectional consistency between visual predictions and action sequences through joint modeling.

As illustrated in Figure 1, AstraNav-World consists of three core components:

- **Vision-Language Model (VLM) Planner**: Serves as the high-level reasoning module that processes instructions and visual history to generate semantic guidance.

- **Video Generator**: Predicts future visual observations based on the VLM's contextual understanding.
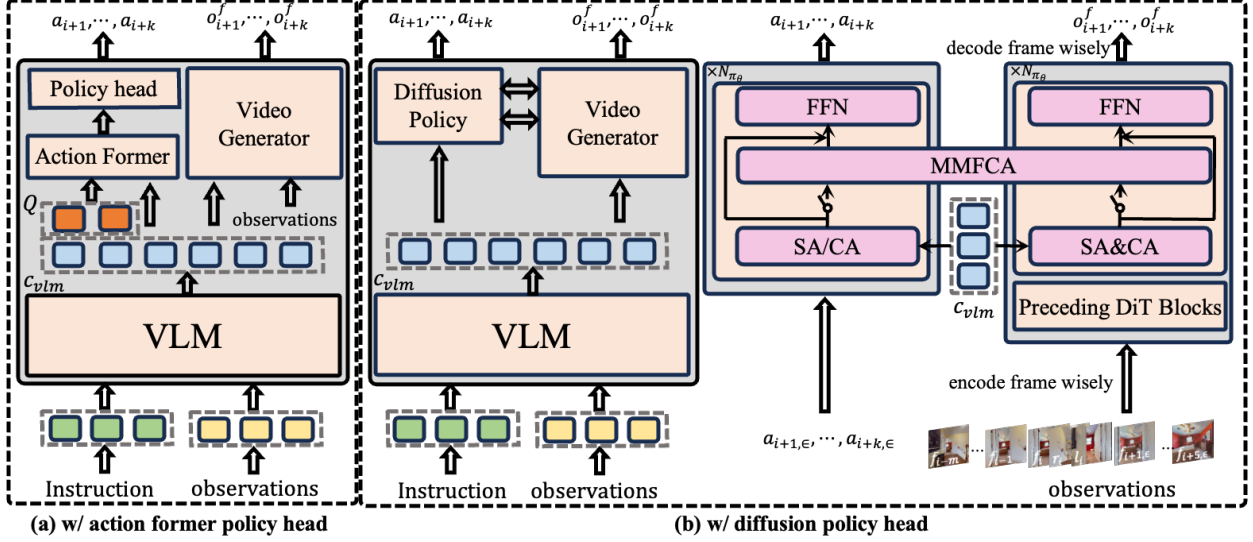
Figure 1 Overview of AstraNav World architecture. Our model adapts to two different policy heads within a unified framework: (a) a traditional policy head with an Action Former for direct action prediction, and (b) a diffusion policy head for probabilistic action generation. These two policy streams share a common VLM planner (τ_θ), which processes instructions and visual history to generate high-level conditional tokens. The architecture also includes a VLM conditional video generator (υ_θ) for predicting and planning consistent future visual scenes. When using diffusion strategy flow, multimodal fusion cross attention (MMFCA) can be selectively used in overlapping DiTBlocks to interconnect, achieving bidirectional information flow between action and visual prediction.

- **Action Policy Head**: Generates future action sequences, implemented through dual policy methods (transformer-based and diffusion-based).

The key innovation is that these components are trained end-to-end with bidirectional constraints, ensuring that:

- VLM understands instructions and makes macro planning.

- Action sequences are grounded in visually plausible futures.

- Visual predictions are consistent with executable actions.

This unified approach eliminates the error accumulation inherent in sequential prediction-planning pipelines, while enabling long-horizon planning with visual foresight. Our model is implemented using Qwen-2.5-VL-3B as the VLM backbone and Wan2.2-TI2V-5B as the foundation for the video generation and policy components.

3.2 VLM as Central Planner

The VLM, denoted as τ_θ, serves as the high-level reasoning core of our agent. At each timestep, it takes as input the natural language instruction I and a sequence of historical visual observations $\mathcal{O}_{\text{hist}} = \{o_{i-k}, \ldots, o_i\}$.

Output Representation The VLM generates a set of **Vision-Language Embeddings**, $C \in \mathbb{R}^{L \times D}$ where L is the sequence length and $D = 2048$ is the embedding dimension. These embeddings contain two key components:

- **Goal-oriented Semantic Features**: Encoded from the instruction, capturing the high-level navigation objective.

- **Spatial Context Features**: Encoding the historical and current visual semantic and spatial features.

These embeddings provide a unified high-level directive for both the action and vision prediction streams, ensuring cohesive planning and prediction. The key is that this representation not only enables the model to maintain a holistic understanding of long-horizon tasks, but also allows it to flexibly adapt to immediate changes in the environment.

3.3 VLM-Conditioned Video Generator

3.3.1 Basic Architecture

Our approach leverages Wan-2.2-TI2V-5B Wan et al. (2025), a bidirectional diffusion-based video generation system initially trained for short video synthesis from text or image inputs. At its core, the architecture integrates two key components: a spatio-temporal variational autoencoder(ST-VAE) and diffusion transformer networks (DiTs). The ST-VAE features a 3D causal structure that efficiently compresses high-resolution video content into a compact latent representation, achieving a $16\times$ spatial compression ratio and a $4\times$ temporal compression ratio. The diffusion process is implemented through a series of diffusion transformers (DiTs) that include patchifying and unpatchifying layers along with 30 transformer blocks. In the original Wan architecture, input text descriptions are encoded with umT5 Chung et al. (2023) and integrated via cross-attention, while denoising timestep embeddings are injected through a shared MLP module. For I2V tasks, the model will concatenate the latent of the input image and noisy latent in the temporal dimension and set corresponding timestep of first frame latent to zero. In our task, we concatenate all observations in the batch dimension instead of the original temporal dimension to avoid temporal compression of ST-VAE and we set corresponding timestep of historical and current latent frames to zero.

3.3.2 VLM planner as Conditional Encoder.

To ensure the predicted future observations are aligned with the VLM's high-level plan, we replace the conventional text encoder of the video model with our VLM planner, τ_θ. The Vision-Language Embeddings from τ_θ are injected into the video diffusion model's DiT architecture via cross-attention layers. This allows the VLM to directly steer the generation process, ensuring the synthesized future frames are semantically consistent with VLM's planning.

3.3.3 3D-RoPE Rearrangement.

Following the original settings, our framework employs 3D Rotary Position Embeddings Su et al. (2024) in DiT blocks. To handle the combined input of historical frames $o_{i-k}, \ldots, o_{i-1}$ (with natural temporal indexing $t_j = j$) and current multi-view observations, we introduce a 3D-RoPE rearrangement strategy. The historical frames maintain standard temporal ordering, the current left, front, and right views at t_i are virtually arranged side-by-side along the width axis, preserving shared temporal and height indices while encoding their spatial-temporal relationships. For a frame with original width W, the coordinate transformation works as follows:

$$PE_{t_i}^{\text{front}} \mapsto (t', h', w') = (t_i, h, w) \tag{1}$$

$$PE_{t_i}^{\text{right}} \mapsto (t', h', w') = (t_i, h, w + W) \tag{2}$$

$$PE_{t_i}^{\text{left}} \mapsto (t', h', w') = (t_i, h, w + 2W) \tag{3}$$

3.3.4 Optimization Objective.

The video generator is trained using a conditional denoising objective specifically designed for navigation context prediction. During training, we apply a differential noise scheduling strategy to distinguish between observed and predicted frames. The historical front perspective frames $o_{i-m}^f, \ldots, o_{i-1}^f$ and the current multi-view observations (o_i^f, o_i^l, o_i^r) are provided with a minimal noise level ($\sigma_{\text{obs}} \approx 0.05$), effectively treating them as clean conditioning inputs. In contrast, the future front perspective frames $o_{i+1}^f, \ldots, o_{i+N}^f$ are trained with noise added by Flow Matching method.

Let $z^{\text{future}} = \mathcal{E}(o^{\text{future}})$ ($\mathcal{E}$ means the encoder of ST-VAE) denote the sequence of latent representations for the ground-truth future frames. For each training iteration, we sample a noise level σ_t and a noise sample $\epsilon \sim \mathcal{N}(0, I)$. The latent state at time t is constructed as $z_t = (1 - t) \cdot z^{\text{future}} + t \cdot \epsilon$, while the conditioning frames (historical and current) remain at a near-zero noise level. The target velocity field is defined as $u_t = \epsilon - z^{\text{future}}$.

The optimization objective focuses exclusively on the future frames, formulated as:

$$\mathcal{L}_{\text{VG}} = \mathbb{E}_{t,z^{\text{future}},C} \left[\left\| v_\theta(z_t, t, C) - (\epsilon - z^{\text{future}}) \right\|^2 \right] \tag{4}$$

where v_θ represents the video generation network, $C = \{c_{\text{vlm}}\}$ contains the VLM planner's contextual embeddings, and the expectation is taken only over the future frames.

3.4 Action Policy Head

3.4.1 Action Former Policy

The first policy implementation employs a query-based Transformer architecture that processes the VLM's contextual embeddings to generate action sequences. This approach utilizes a fixed set of N_q learnable query vectors $Q \in \mathbb{R}^{N_q \times D}$ that are initialized randomly and updated during training. These queries interact with the VLM's output embeddings $E_{\text{vlm}} \in \mathbb{R}^{L \times D}$ through a multi-layer Transformer encoder, consisting of N_{enc} stacked blocks with multi-head self-attention and feed-forward networks. Then the queries can capture temporal dependencies and contextual relationships and produce refined query representations $Q' \in \mathbb{R}^{N_q \times D}$. These representations are then passed through a multi-layer perceptron (MLP) head that maps each query to a step of action in the navigation space, yielding the predicted action sequence $A = \{a_{i+1}, \dots, a_{i+N}\}$. This architecture provides an efficient mechanism for deterministic action generation while maintaining computational efficiency.

The Action Former policy generates actions represented as $A = (X, Y, \cos(\theta), \sin(\theta), \alpha)$, where (X, Y) denote the relative position displacement, $(\cos(\theta), \sin(\theta))$ encode the heading angle in a rotationally invariant manner, and α is a binary flag indicating arrival at the target.

The loss function is composed of three distinct components that address different aspects of the navigation task:

- **Position Loss**: For the (X, Y) components, we apply L1 loss to measure the absolute error between predicted and ground-truth displacements:

$$\mathcal{L}_{\text{pos}} = \frac{1}{N} \sum_{n=1}^{N} \left(|X_n - X_n^*| + |Y_n - Y_n^*| \right) \tag{5}$$

- **Angle Loss**: The heading angle is optimized using cosine similarity between the predicted and ground-truth direction vectors:

$$\mathcal{L}_{\text{angle}} = 1 - \frac{1}{N} \sum_{n=1}^{N} \left(\cos(\theta_n) \cos(\theta_n^*) + \sin(\theta_n) \sin(\theta_n^*) \right) \tag{6}$$

This formulation ensures rotational consistency and avoids the discontinuity issues that would occur with direct angle regression.

- **Arrival Loss**: The arrival flag is optimized using binary cross-entropy with logits:

$$\mathcal{L}_{\text{arrive}} = -\frac{1}{N} \sum_{n=1}^{N} \left[\alpha_n^* \log(\sigma(\alpha_n)) + (1 - \alpha_n^*) \log(1 - \sigma(\alpha_n)) \right] \tag{7}$$

where σ denotes the sigmoid function.

The total loss for the Action Former policy is a weighted combination:

$$\mathcal{L}_{\text{PH}} = \lambda_1 \mathcal{L}_{\text{pos}} + \lambda_2 \mathcal{L}_{\text{angle}} + \lambda_3 \mathcal{L}_{\text{arrive}} \tag{8}$$

with $\lambda_1 = 1.0$, $\lambda_2 = 1.0$, and $\lambda_3 = 1.0$ empirically determined to balance the contributions of each component. This multi-objective formulation ensures that the policy simultaneously optimizes for accurate position prediction, correct orientation, and appropriate termination conditions.

3.4.2 Diffusion Policy

The second policy implementation adopts a diffusion-based approach that generates actions through a denoising process, providing probabilistic action predictions that better capture the uncertainty inherent in navigation tasks. Each block contains one attention and one FFN, with self-attention and cross-attention alternately. The diffusion policy operates on noisy action sequences A_t and gradually refines them to produce clean, executable trajectories. A key innovation in this implementation is the integration of the Multimodal Fusion Cross-Attention (MMFCA) module between the last 8 overlapping blocks (with cross attention) of the diffusion policy and video generator streams. The MMFCA enables bidirectional information flow through dual cross-attention operations:

- **Action-to-Video Attention**: The refined action representations serve as queries (Q_A) that attend to the video latent representations (K_V, V_V), ensuring actions are grounded in visually plausible futures

- **Video-to-Action Attention**: The video latent representations serve as queries (Q_V) that attend to the action representations (K_A, V_A), ensuring visual predictions remain causally consistent with the planned actions

The MMFCA module is controlled by a binary switch $\gamma \in \{0, 1\}$. When $\gamma = 1$ we enable bidirectional fusion between the video generator and the policy via MMFCA module, so that video prediction and action generation are coupled and can be produced synchronously within the same rollout. When $\gamma = 0$ the fusion is disabled and the two streams operate independently; in particular, for efficient inference, we can skip the video generator entirely and run only the policy to predict actions, which substantially reduces computation.

The Diffusion Policy is trained using Flow Matching method Lipman et al. (2022); Liu et al. (2022), a continuous-time diffusion framework that learns to predict the velocity field that transports noise to the target distribution. Given a ground-truth action sequence A_{future} and a noise sample $\epsilon \sim \mathcal{N}(0, I)$, we construct a linear interpolation path $A_t = (1 - t) \cdot A_{\text{future}} + t \cdot \epsilon$. The target velocity field is defined as $v_t = \epsilon - A_{\text{future}}$.

The loss function for the Diffusion Policy is formulated as:

$$\mathcal{L}_{\text{PH}} = \mathbb{E}_{t, A_{\text{future}}, \epsilon, C} \left[\|v_{\phi,\theta}(A_t, t, C) - (\epsilon - A_{\text{future}})\|^2 \right] \tag{9}$$

where $v_{\phi,\theta}$ denotes the velocity prediction network, and C represents the VLM planner's contextual embeddings.

3.5 Speed Optimization

The intrinsic speed of video generation, particularly with diffusion transformer models , can be a bottleneck for real-time navigation tasks that demand high-frequency actions. To address this, we propose **Sparse Foresight Scheduling** (SFS). Through joint modeling and joint training, the VLM possesses sufficiently strong planning and generalization capabilities, extending these capabilities to the policy level. So Instead of generating a future frame and action at every single time step, we perform this joint generation process at fixed, pre-determined intervals. This is a pragmatic decision, as many navigation scenarios involve prolonged periods of simple, consistent behaviors such as straight-line movement, which do not necessitate instantaneous updates to the world model. By generating future predictions only at these sampled intervals, we significantly reduce computational overhead and save valuable time.

During inference, our system adapts its computational strategy based on the selected policy head. When utilizing the Action Former policy head, we completely deactivate the video generator, relying solely on the query-based Transformer architecture to generate action sequences without visual prediction.

Because we disabled MMFCA for 50% of the training process, our diffusion policy has sufficient independence to allow us to intermittently disable joint prediction and only predict future actions. For the Diffusion Policy head, we activate the video generator only at fixed interval steps (every 10 steps in our implementation), while keeping it deactivated during intermediate steps. This selective activation approach allows our model to benefit from visual foresight when it matters most while significantly reducing computational overhead, achieving an optimal trade-off between predictive accuracy and inference speed.

4 Experiments

4.1 Data Process

Our data resources encompass two types of navigation tasks: instruction-goal navigation and object-goal navigation.

Instruction-goal navigation data. Under Habitat's continuous environment configuration (VLN-CE) and Matterport3D indoor scenes Chang et al. (2017), we construct navigation episodes based on the public instruction–path pairs from R2R Anderson et al. (2018b) and RxR Ku et al. (2020). For each trajectory, we store multimodal information, including a panoramic sequence composed of three camera views (left, front, right), the corresponding sequences of discrete actions and continuous waypoints, and the paired natural-language instruction.

Object-goal navigation data. Following the open-vocabulary object navigation setting (OVON) Yokoyama et al. (2024b), we randomly sample (start pose, target object category) pairs in HM3D scenes Ramakrishnan et al. (2021).

A built-in shortest-path planner guides the agent to the vicinity of the target to generate samples, and we record each episode in the same format as the instruction-goal data (three-view panoramic frames, discrete action and continuous waypoint sequences, and the associated textual description).

Navigation data Process. Navigation comprises four discrete action types (forward, left, right, stop). Each action step corresponds to a continuous trajectory point composed of position and orientation: position is a 3D coordinate (X, Y, Z), and rotation is a quaternion (w, x, y, z). During trajectory prediction, we first convert each 6-DoF pose to a local coordinate frame: the current front-view frame serves as the origin and heading reference, and all other trajectory points are transformed relative to this reference. We then project the 3D pose onto the ground plane, retaining (X, Y) and the heading angle θ, and add an "arrival" flag α at each step. Finally, each trajectory point (action) is represented as a quadruple (X,Y,θ,α), namely $A=(X,Y,\theta,\alpha)$, which serves as the primary action optimization target.

4.2 Implementation Details

For the Vision-Language Model, we utilize **Qwen2.5-VL-3B** and perform full-parameter supervised fine-tuning. The video generator is based on **Wan2.2-TI2V-5B** and is fine-tuned using the LoRA method with both rank and scale set to 128. Empirical observations indicate that LoRA training offers superior stability and convergence speed for the video module. For the policy components, we implement two distinct variants: (i) The **Action Former** variant employs 5 learnable query embeddings processed through 4 stacked Transformer blocks to predict deterministic trajectories. (ii) The **Diffusion Policy** variant utilizes a deeper architecture with 16 Transformer layers. Furthermore, we integrate the MMFCA module between the Diffusion Policy and the final 8 blocks (with cross attention) of the video generator to facilitate deep cross-modal interactions. We set the learning rate to 1×10^{-5} and adopt a cosine decay schedule. All experiments are conducted on a cluster equipped with 96 H20 GPUs.

4.2.1 VLM pretraining

To endow our central planner with broad world knowledge and robust reasoning capabilities, we initialize the Vision-Language Model (VLM), τ_θ, from a checkpoint pretrained on a diverse mixture of large-scale, general-purpose vision-language datasets. These datasets cover fundamental tasks such as Visual Question Answering (VQA) and object grounding, which provide the model with a foundational understanding of object semantics and spatial relationships and instruction comprehension. In addition, the navigation dataset of R2R, RxR and Ovon as described above are also added to pretrain the VLM in an autoregressive way following the work of OmniNav Xue et al. (2025). This pretraining process ensures that the VLM is not only a knowledgeable reasoner but also an expert planner adapted to the visual features and action-oriented instructions.

4.2.2 Video-Action Prediction Training

The training of AstraNav-World follows a two-stage training strategy designed to effectively leverage pre-trained components while optimizing the complex interactions between visual and action prediction.

Total loss The overall training objective combines the video generator loss ($\mathcal{L}_{\text{VG}}$) and policy head loss ($\mathcal{L}_{\text{PH}}$) into a unified framework:

$$\mathcal{L}_{\text{Total}} = \mathcal{L}_{\text{VG}} + \lambda \mathcal{L}_{\text{PH}} \tag{10}$$

where $\lambda = 1.0$ is the balancing coefficient empirically determined to optimize the trade-off between visual prediction accuracy and action prediction quality.

Training Strategy Our training process consists of two carefully designed stages:

Stage 1: Component-Specific Pretraining. The VLM planner is initialized from a checkpoint pretrained on large-scale vision-language datasets and kept frozen during this entire stage. We first train the video generator independently using $\mathcal{L}_{\text{VG}}$, with the Flow Matching objective focusing exclusively on future frame prediction. Subsequently, we train the policy head independently using $\mathcal{L}_{\text{PH}}$, optimizing for both position accuracy and action semantics. This stage provides strong initializations for both components while avoiding early optimization conflicts and ensuring each module develops its core capabilities before integration.

Table 1 Main comparison with prior methods on the Val-Unseen split of R2R-CE and RxR-CE (vg indicates video-generator, * indicates methods using the waypoint predictor).

Method	Observation				R2R-CE Val-Unseen				RxR-CE Val-Unseen		
	S.RGB	Pano.	Depth	Odo.	NE↓	OS↑	SR↑	SPL↑	NE↓	SR↑	SPL↑
HPN+DN* (Krantz et al., 2021)		✓	✓	✓	6.31	40.0	36.0	34.0	-	-	-
CMA* (Hong et al., 2022)		✓	✓	✓	6.20	52.0	41.0	36.0	8.76	26.5	22.1
Sim2Sim* (Krantz and Lee, 2022)		✓	✓	✓	6.07	52.0	43.0	36.0	-	-	-
GridMM* (Wang et al., 2023b)		✓	✓	✓	5.11	61.0	49.0	41.0	-	-	-
DreamWalker* (Wang et al., 2023a)		✓	✓	✓	5.53	59.0	49.0	44.0	-	-	-
Reborn* (An et al., 2022)		✓	✓	✓	5.40	57.0	50.0	46.0	5.98	48.6	42.0
ETPNav* (An et al., 2024)		✓	✓	✓	4.71	65.0	57.0	49.0	5.64	54.7	44.8
HNR* (Wang et al., 2024)		✓	✓	✓	4.42	67.0	61.0	51.0	5.50	56.3	46.7
AG-CMTP (Chen et al., 2021)		✓	✓	✓	7.90	39.0	23.0	19.0	-	-	-
R2R-CMTP (Chen et al., 2021)		✓	✓	✓	7.90	38.0	26.0	22.0	-	-	-
InstructNav (Long et al., 2024)		✓	✓	✓	6.89	-	31.0	24.0	-	-	-
LAW (Raychaudhuri et al., 2021)	✓		✓	✓	6.83	44.0	35.0	31.0	10.90	8.0	8.0
CM2 (Georgakis et al., 2022)	✓		✓	✓	7.02	41.0	34.0	27.0	-	-	-
WS-MGMap (Chen et al., 2022)	✓		✓	✓	6.28	47.0	38.0	34.0	-	-	-
AO-Planner (Chen et al., 2025)		✓	✓		5.55	59.0	47.0	33.0	7.06	43.3	30.5
Seq2Seq (Krantz et al., 2020)	✓		✓		7.77	37.0	25.0	22.0	12.10	13.9	11.9
CMA (Krantz et al., 2020)	✓		✓		7.37	40.0	32.0	30.0	-	-	-
NaVid (Zhang et al., 2024b)	✓				5.47	49.0	37.0	35.0	-	-	-
Uni-NaVid (Zhang et al., 2024a)	✓				5.58	53.5	47.0	42.7	6.24	48.7	40.9
NaVILA (Cheng et al., 2024)	✓				5.22	62.5	54.0	49.0	6.77	49.3	44.0
StreamVLN (Wei et al., 2025)	✓				4.98	64.2	56.9	51.9	6.22	52.9	46.0
CorrectNav (Yu et al., 2025)	✓				4.24	67.5	65.1	62.3	4.09	69.3	63.3
AstraNav-World w/ Action Former		✓			3.93	73.1	67.2	64.2	3.93	70.4	59.6
AstraNav-World w/ Diffusion Policy		✓			**3.86**	**73.9**	**67.9**	**65.4**	**3.82**	**72.9**	**61.5**

Stage 2: Joint Fine-tuning. In this stage, we unfreeze all components and jointly optimize the entire model with $\mathcal{L}_{\text{Total}}$. For models using the Diffusion Policy head, we randomly enable the MMFCA module with 50% probability during training, which ensures the policy develops robust standalone capabilities while maintaining the ability to leverage visual guidance when available. This selective activation strategy prevents over-reliance on visual feedback and guarantees the diffusion policy can operate effectively even when visual information is limited or when the video generator is deactivated during inference for computational efficiency.

Table 2 Evaluation of object-goal navigation on HM3D-OVON.

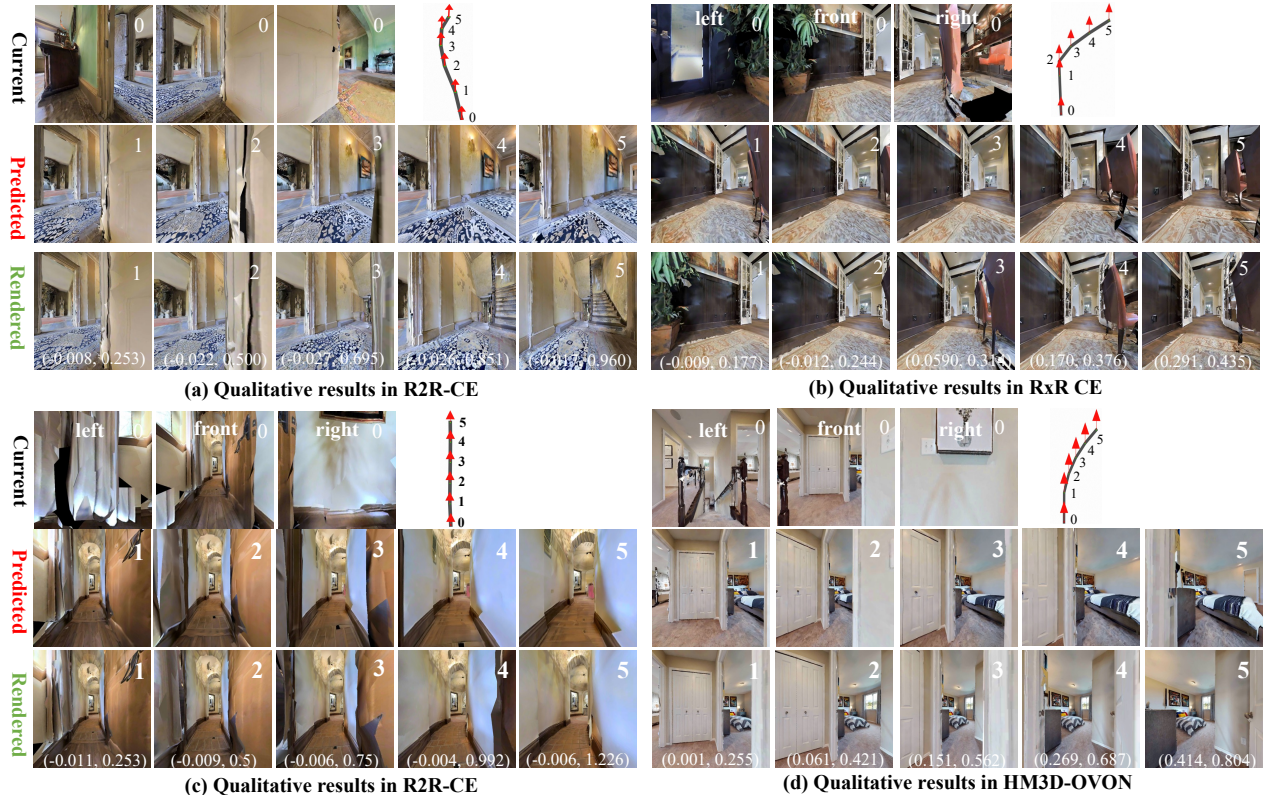| Method	Val-Unseen	
	SR↑	SPL↑
VLFM (Yokoyama et al., 2024a)	35.2	19.6
DAgRL+OD (Yokoyama et al., 2024b)	37.1	19.8
Uni-NaVid (Zhang et al., 2024a)	39.5	19.8
MTU3D (Zhu et al., 2025b)	40.8	12.1
AstraNav-World w/ Action Former	45.1	28.3
AstraNav-World w/ Diffusion Policy	**45.7**	**28.7**

Figure 2 Qualitative results. Our model predict the next five visual frames while simultaneously outputting the corresponding 5-step waypoint sequence. The generated frames are in strong agreement with the scenes rendered from the predicted waypoints and also the predicted trajectory marked with red arrows, showing strong consistency.

4.3 Main Results

4.3.1 Metric Comparison

We assess navigation performance using four standard metrics: success rate (SR), oracle success (OS), success weighted by path length (SPL), and navigation error (NE). Our evaluation setup mirrors established practice in the literature and follows the protocols used in prior work Zhang et al. (2024a); Zhu et al. (2025b). Across instruction-following benchmarks R2R-CE and RxR-CE, AstraNav-World demonstrates significant improvements with both policy variants. The Action Former policy achieves a 2.1% absolute improvement in success rate over prior methods on R2R-CE and 1.1% on RxR-CE. The Diffusion Policy with MMFCA further enhances performance, delivering an additional 0.7% gain on R2R-CE and 2.5% on RxR-CE compared to the Action Former variant (see Tables 1). For open-vocabulary object navigation on HM3D-OVON, the Diffusion Policy variant shows the strongest results with a 4.9% absolute improvement over previous state-of-the-art, while the Action Former policy achieves a 4.3% improvement (see Table 2).

4.3.2 Abaltion Study

To assess the effectiveness of our approach, we conduct a series of controlled ablation studies, as shown in Fig. 3(a). We disable the video generator and train the diffusion policy variant. We then evaluate navigation performance on R2R, RxR, and OVON using Success Rate (SR). Across all datasets, removing the video generator leads to a consistent drop in SR, confirming that explicitly predicting future visual observations provides more informative guidance for planning and substantially improves navigation accuracy.

We further ablate the proposed SFS on R2R (randomly select 100 cases) to understand its impact on efficiency and performance, as shown in Fig. 3(b). We compare three SFS configurations with different fixed skipping intervals and report their inference time and SR. As the skipping interval increases, inference becomes up to an order of magnitude faster, while SR remains almost unchanged.
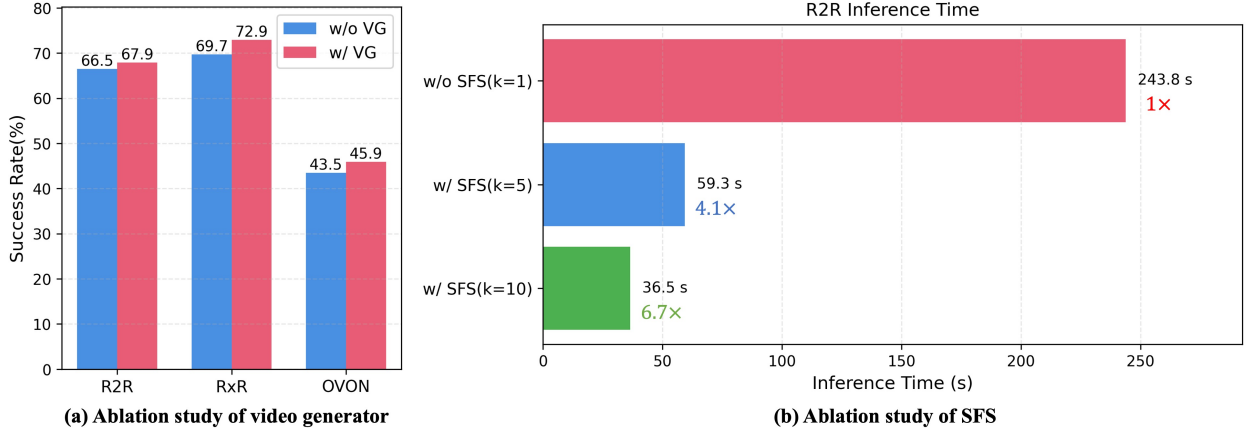
(a) Ablation study of video generator   **(b) Ablation study of SFS**

Figure 3 Ablation study results. (a) **Impact of the video generator (VG):** Comparing the Success Rate (SR) with and without VG across R2R, RxR, and OVON datasets shows that predicting future observations consistently improves navigation performance. (b) **Efficiency of SFS:** Evaluation of the proposed SFS strategy on R2R with different skipping intervals k. The results demonstrate that increasing k significantly reduces inference time (up to $6.7\times$ speedup) while maintaining robust performance.

Table 3 Comparison of PSNR and FVD on R2R and RxR.

Dataset	Method	PSNR ↑	FVD ↓
R2R	5-step	13.69	670
	1-step	15.54	–
RxR	5-step	14.50	497
	1-step	18.55	–

4.3.3 Consistency Analysis

As shown in Figure 2, the future views generated by the video generator exhibit strong qualitative consistency with the waypoint-rendered results, closely coupling visual appearance and motion trends with the planned trajectory in both straight and turning scenarios. Specifically, camera translation and rotation accurately reflect waypoint motion, and macro-geometric cues like object contours and orientations align with the planned layout. To quantitatively validate this consistency, as presented in Table 3, we sampled 500 instances using a diffusion policy variant and calculated the PSNR and FVD between the predicted future five frames (and future one frame) and the actual viewpoints. The strong performance in these metrics further confirms the successful training of our video model and its ability to generate visually coherent and geometrically aligned future frames.

4.3.4 Real World Testing

To evaluate the real-world applicability of our approach, we conducted testing of AstraNav-World on a physical robot platform without any retraining or fine-tuning on real-world data. The testing involved several navigation tasks across real-world environment, where the robot was tasked with following natural language instructions to reach specific locations or interact with objects. Despite the significant domain gap between simulation and reality, AstraNav-World achieved good results on these real-world tasks, substantially outperforming prior methods that typically require domain adaptation (refer to the project page).

Qualitative analysis revealed that the model's ability to generate future visual predictions enabled it to anticipate challenging transitions such as doorway passages and corner turns, significantly improving navigation robustness. This remarkable zero-shot transfer capability validates the fundamental advantage of world modeling approaches: by learning the underlying physical and navigational principles rather than simply fitting data distributions in simulation environment, our model captures essential spatial relationships and dynamics that generalize across domains. These results establish AstraNav-World as one of the first navigation models to achieve competitive real-world performance without any real-world training data, demonstrating the true potential of generative world models for embodied navigation.

5 Conclusion

This paper addresses core issues in embodied navigation caused by the loosely coupled "envision-then-plan" paradigm, including physical and causal inconsistency and error accumulation, by proposing a unified generative world model for navigation, AstraNav-World. It tightly binds "envision the future" and "plan the future" within a single probabilistic framework. Centered on a VLM with long-horizon understanding as the planner, the framework integrates future visual prediction with action planning through two different approaches: an Action Former policy for deterministic action generation and a diffusion policy with MMFCA for probabilistic action prediction. To handle multi-view inputs, we introduce a 3D-RoPE rearrangement method that maintains precise spatial-temporal alignment for current frames from different camera perspectives. The model is trained through a two-stage process that first develops strong individual capabilities through staged pretraining, followed by end-to-end joint optimization to enhance both executability and robustness.

Experiments show that AstraNav-World leads on the R2R-CE, RxR-CE, and HM3D-OVON navigation benchmarks with both policy variants; removing the video generation branch results in metric degradation for both implementations. Notably, our framework demonstrates exceptional generalization capabilities, with models trained exclusively in simulation achieving strong performance in real-world environments, validating the world model's ability to capture fundamental physical and navigational principles. Qualitative analysis indicates that the generated future viewpoints are highly consistent with the pose changes along the planned trajectory, markedly improving decision interpretability. To balance real-time performance, we adopt time-sliced inference so that video generation and the diffusion policy collaborate at fixed intervals, maintaining accuracy while reducing computational overhead.

AstraNav-World uses a strong VLM, physics-consistent video generation, and task-aligned policy prediction to produce coherent, executable long-horizon navigation plans. Challenges include generation latency and compute limits in complex scenes. Future work will scale to longer horizons and harder tasks, strengthen physical and causal world modeling, improve closed-loop consistency and real-time reasoning/planning, and make embodied agents more reliable and interpretable in the real world.

References

Arslan Ali, Junjie Bai, Maciej Bala, Yogesh Balaji, Aaron Blakeman, Tiffany Cai, Jiaxin Cao, Tianshi Cao, Elizabeth Cha, Yu-Wei Chao, et al. World simulation with video foundation models for physical ai. *arXiv preprint arXiv:2511.00062*, 2025.

Dong An, Zun Wang, Yangguang Li, Yi Wang, Yicong Hong, Yan Huang, Liang Wang, and Jing Shao. 1st place solutions for rxr-habitat vision-and-language navigation competition (cvpr 2022). *arXiv preprint arXiv:2206.11610*, 2022.

Dong An, Hanqing Wang, Wenguan Wang, Zun Wang, Yan Huang, Keji He, and Liang Wang. Etpnav: Evolving topological planning for vision-language navigation in continuous environments. *IEEE Transactions on Pattern Analysis and Machine Intelligence*, 2024.

Peter Anderson, Angel Chang, Devendra Singh Chaplot, Alexey Dosovitskiy, Saurabh Gupta, Vladlen Koltun, Jana Kosecka, Jitendra Malik, Roozbeh Mottaghi, Manolis Savva, et al. On evaluation of embodied navigation agents. *arXiv preprint arXiv:1807.06757*, 2018a.

Peter Anderson, Qi Wu, Damien Teney, Jake Bruce, Mark Johnson, Niko Sünderhauf, Ian Reid, Stephen Gould, and Anton Van Den Hengel. Vision-and-language navigation: Interpreting visually-grounded navigation instructions in real environments. In *Proceedings of the IEEE conference on computer vision and pattern recognition*, pages 3674–3683, 2018b.

Shuai Bai, Keqin Chen, Xuejing Liu, Jialin Wang, Wenbin Ge, Sibo Song, Kai Dang, Peng Wang, Shijie Wang, Jun Tang, et al. Qwen2. 5-vl technical report. *arXiv preprint arXiv:2502.13923*, 2025.

Amir Bar, Gaoyue Zhou, Danny Tran, Trevor Darrell, and Yann LeCun. Navigation world models. In *Proceedings of the Computer Vision and Pattern Recognition Conference*, pages 15791–15801, 2025.

Jake Bruce, Michael D Dennis, Ashley Edwards, Jack Parker-Holder, Yuge Shi, Edward Hughes, Matthew Lai, Aditi Mavalankar, Richie Steigerwald, Chris Apps, et al. Genie: Generative interactive environments. In *Forty-first International Conference on Machine Learning*, 2024.

Jun Cen, Chaohui Yu, Hangjie Yuan, Yuming Jiang, Siteng Huang, Jiayan Guo, Xin Li, Yibing Song, Hao Luo, Fan Wang, et al. Worldvla: Towards autoregressive action world model. *arXiv preprint arXiv:2506.21539*, 2025.

Angel Chang, Angela Dai, Thomas Funkhouser, Maciej Halber, Matthias Niessner, Manolis Savva, Shuran Song, Andy Zeng, and Yinda Zhang. Matterport3d: Learning from rgb-d data in indoor environments. *arXiv preprint arXiv:1709.06158*, 2017.

Chi-Lam Cheang, Guangzeng Chen, Ya Jing, Tao Kong, Hang Li, Yifeng Li, Yuxiao Liu, Hongtao Wu, Jiafeng Xu, Yichu Yang, et al. Gr-2: A generative video-language-action model with web-scale knowledge for robot manipulation. *arXiv preprint arXiv:2410.06158*, 2024.

Jiaqi Chen, Bingqian Lin, Xinmin Liu, Lin Ma, Xiaodan Liang, and Kwan-Yee K Wong. Affordances-oriented planning using foundation models for continuous vision-language navigation. In *Proceedings of the AAAI Conference on Artificial Intelligence*, volume 39, pages 23568–23576, 2025.

Kevin Chen, Junshen K Chen, Jo Chuang, Marynel Vázquez, and Silvio Savarese. Topological planning with transformers for vision-and-language navigation. In *Proceedings of the IEEE/CVF Conference on Computer Vision and Pattern Recognition*, pages 11276–11286, 2021.

Peihao Chen, Dongyu Ji, Kunyang Lin, Runhao Zeng, Thomas Li, Mingkui Tan, and Chuang Gan. Weakly-supervised multi-granularity map learning for vision-and-language navigation. *Advances in Neural Information Processing Systems*, 35:38149–38161, 2022.

An-Chieh Cheng, Yandong Ji, Zhaojing Yang, Zaitian Gongye, Xueyan Zou, Jan Kautz, Erdem Bıyık, Hongxu Yin, Sifei Liu, and Xiaolong Wang. Navila: Legged robot vision-language-action model for navigation. *arXiv preprint arXiv:2412.04453*, 2024.

Hyung Won Chung, Noah Constant, Xavier Garcia, Adam Roberts, Yi Tay, Sharan Narang, and Orhan Firat. Unimax: Fairer and more effective language sampling for large-scale multilingual pretraining. *arXiv preprint arXiv:2304.09151*, 2023.

Chelsea Finn and Sergey Levine. Deep visual foresight for planning robot motion. In *2017 IEEE international conference on robotics and automation (ICRA)*, pages 2786–2793. IEEE, 2017.

Georgios Georgakis, Karl Schmeckpeper, Karan Wanchoo, Soham Dan, Eleni Miltsakaki, Dan Roth, and Kostas Daniilidis. Cross-modal map learning for vision and language navigation. In *Proceedings of the IEEE/CVF conference on computer vision and pattern recognition*, pages 15460–15470, 2022.

Junliang Guo, Yang Ye, Tianyu He, Haoyu Wu, Yushu Jiang, Tim Pearce, and Jiang Bian. Mineworld: a real-time and open-source interactive world model on minecraft. *arXiv preprint arXiv:2504.08388*, 2025.

Xianglong He, Chunli Peng, Zexiang Liu, Boyang Wang, Yifan Zhang, Qi Cui, Fei Kang, Biao Jiang, Mengyin An, Yangyang Ren, et al. Matrix-game 2.0: An open-source, real-time, and streaming interactive world model. *arXiv preprint arXiv:2508.13009*, 2025.

Yicong Hong, Zun Wang, Qi Wu, and Stephen Gould. Bridging the gap between learning in discrete and continuous environments for vision-and-language navigation. In *Proceedings of the IEEE/CVF conference on computer vision and pattern recognition*, pages 15439–15449, 2022.

Yuhang Huang, JIazhao Zhang, Shilong Zou, XInwang Liu, Ruizhen Hu, and Kai Xu. Ladi-wm: A latent diffusion-based world model for predictive manipulation. *arXiv preprint arXiv:2505.11528*, 2025.

Jacob Krantz and Stefan Lee. Sim-2-sim transfer for vision-and-language navigation in continuous environments. In *European conference on computer vision*, pages 588–603. Springer, 2022.

Jacob Krantz, Erik Wijmans, Arjun Majumdar, Dhruv Batra, and Stefan Lee. Beyond the nav-graph: Vision-and-language navigation in continuous environments. In *European Conference on Computer Vision*, pages 104–120. Springer, 2020.

Jacob Krantz, Aaron Gokaslan, Dhruv Batra, Stefan Lee, and Oleksandr Maksymets. Waypoint models for instruction-guided navigation in continuous environments. In *Proceedings of the IEEE/CVF International Conference on Computer Vision*, pages 15162–15171, 2021.

Alexander Ku, Peter Anderson, Roma Patel, Eugene Ie, and Jason Baldridge. Room-across-room: Multilingual vision-and-language navigation with dense spatiotemporal grounding. *arXiv preprint arXiv:2010.07954*, 2020.

Yaron Lipman, Ricky TQ Chen, Heli Ben-Hamu, Maximilian Nickel, and Matt Le. Flow matching for generative modeling. *arXiv preprint arXiv:2210.02747*, 2022.

Xingchao Liu, Chengyue Gong, and Qiang Liu. Flow straight and fast: Learning to generate and transfer data with rectified flow. *arXiv preprint arXiv:2209.03003*, 2022.

Yuxing Long, Wenzhe Cai, Hongcheng Wang, Guanqi Zhan, and Hao Dong. Instructnav: Zero-shot system for generic instruction navigation in unexplored environment. *arXiv preprint arXiv:2406.04882*, 2024.

Jiangran Lyu, Ziming Li, Xuesong Shi, Chaoyi Xu, Yizhou Wang, and He Wang. Dywa: Dynamics-adaptive world action model for generalizable non-prehensile manipulation. *arXiv preprint arXiv:2503.16806*, 2025.

J Bjorck Nvidia, Fernando Castaneda, N Cherniadev, X Da, R Ding, L Fan, Y Fang, D Fox, F Hu, S Huang, et al. Gr00t n1: An open foundation model for generalist humanoid robots. *arXiv preprint arXiv:2503.14734*, 2025.

J Parker-Holder, P Ball, J Bruce, V Dasagi, K Holsheimer, C Kaplanis, A Moufarek, G Scully, J Shar, J Shi, et al. Genie 2: A large-scale foundation world model. *URL: https://deepmind. google/discover/blog/genie-2-a-large-scale-foundation-world-model*, 2024.

Santhosh K Ramakrishnan, Aaron Gokaslan, Erik Wijmans, Oleksandr Maksymets, Alex Clegg, John Turner, Eric Undersander, Wojciech Galuba, Andrew Westbury, Angel X Chang, et al. Habitat-matterport 3d dataset (hm3d): 1000 large-scale 3d environments for embodied ai. *arXiv preprint arXiv:2109.08238*, 2021.

Sonia Raychaudhuri, Saim Wani, Shivansh Patel, Unnat Jain, and Angel X Chang. Language-aligned waypoint (law) supervision for vision-and-language navigation in continuous environments. *arXiv preprint arXiv:2109.15207*, 2021.

Lloyd Russell, Anthony Hu, Lorenzo Bertoni, George Fedoseev, Jamie Shotton, Elahe Arani, and Gianluca Corrado. Gaia-2: A controllable multi-view generative world model for autonomous driving. *arXiv preprint arXiv:2503.20523*, 2025.

Yu Shang, Yangcheng Yu, Xin Zhang, Xin Jin, Haisheng Su, Wei Wu, and Yong Li. Mowm: Mixture-of-world-models for embodied planning via latent-to-pixel feature modulation. *arXiv preprint arXiv:2509.21797*, 2025.

Jianlin Su, Murtadha Ahmed, Yu Lu, Shengfeng Pan, Wen Bo, and Yunfeng Liu. Roformer: Enhanced transformer with rotary position embedding. *Neurocomputing*, 568:127063, 2024.

GigaBrain Team, Angen Ye, Boyuan Wang, Chaojun Ni, Guan Huang, Guosheng Zhao, Haoyun Li, Jie Li, Jiagang Zhu, Lv Feng, et al. Gigabrain-0: A world model-powered vision-language-action model. *arXiv preprint arXiv:2510.19430*, 2025.

Yan Team. Yan: Foundational interactive video generation. *arXiv preprint arXiv:2508.08601*, 2025.

Team Wan, Ang Wang, Baole Ai, Bin Wen, Chaojie Mao, Chen-Wei Xie, Di Chen, Feiwu Yu, Haiming Zhao, Jianxiao Yang, et al. Wan: Open and advanced large-scale video generative models. *arXiv preprint arXiv:2503.20314*, 2025.

Hanqing Wang, Wei Liang, Luc V Gool, and Wenguan Wang. Towards versatile embodied navigation. *Advances in neural information processing systems*, 35:36858–36874, 2022.

Hanqing Wang, Wei Liang, Luc Van Gool, and Wenguan Wang. Dreamwalker: Mental planning for continuous vision-language navigation. In *Proceedings of the IEEE/CVF international conference on computer vision*, pages 10873–10883, 2023a.

Shaoan Wang, Jiazhao Zhang, Minghan Li, Jiahang Liu, Anqi Li, Kui Wu, Fangwei Zhong, Junzhi Yu, Zhizheng Zhang, and He Wang. Trackvla: Embodied visual tracking in the wild. *arXiv preprint arXiv:2505.23189*, 2025.

Zihan Wang, Xiangyang Li, Jiahao Yang, Yeqi Liu, and Shuqiang Jiang. Gridmm: Grid memory map for vision-and-language navigation. In *Proceedings of the IEEE/CVF International conference on computer vision*, pages 15625–15636, 2023b.

Zihan Wang, Xiangyang Li, Jiahao Yang, Yeqi Liu, Junjie Hu, Ming Jiang, and Shuqiang Jiang. Lookahead exploration with neural radiance representation for continuous vision-language navigation. In *Proceedings of the IEEE/CVF conference on computer vision and pattern recognition*, pages 13753–13762, 2024.

Meng Wei, Chenyang Wan, Xiqian Yu, Tai Wang, Yuqiang Yang, Xiaohan Mao, Chenming Zhu, Wenzhe Cai, Hanqing Wang, Yilun Chen, et al. Streamvln: Streaming vision-and-language navigation via slowfast context modeling. *arXiv preprint arXiv:2507.05240*, 2025.

Yuchen Wu, Pengcheng Zhang, Meiying Gu, Jin Zheng, and Xiao Bai. Embodied navigation with multi-modal information: A survey from tasks to methodology. *Information Fusion*, 112:102532, 2024.

Jingqiao Xiu, Fangzhou Hong, Yicong Li, Mengze Li, Wentao Wang, Sirui Han, Liang Pan, and Ziwei Liu. Egotwin: Dreaming body and view in first person. *arXiv preprint arXiv:2508.13013*, 2025.

Xinda Xue, Junjun Hu, Minghua Luo, Xie Shichao, Jintao Chen, Zixun Xie, Quan Kuichen, Guo Wei, Mu Xu, and Zedong Chu. Omninav: A unified framework for prospective exploration and visual-language navigation. *arXiv preprint arXiv:2509.25687*, 2025.

Kai Yang, Tianlin Zhang, Zhengbo Wang, Zedong Chu, Xiaolong Wu, Yang Cai, and Mu Xu. Ce-nav: Flow-guided reinforcement refinement for cross-embodiment local navigation, 2025. https://arxiv.org/abs/2509.23203.

Xuan Yao, Junyu Gao, and Changsheng Xu. Navmorph: A self-evolving world model for vision-and-language navigation in continuous environments. *arXiv preprint arXiv:2506.23468*, 2025.

Naoki Yokoyama, Sehoon Ha, Dhruv Batra, Jiuguang Wang, and Bernadette Bucher. Vlfm: Vision-language frontier maps for zero-shot semantic navigation. In *2024 IEEE International Conference on Robotics and Automation (ICRA)*, pages 42–48. IEEE, 2024a.

Naoki Yokoyama, Ram Ramrakhya, Abhishek Das, Dhruv Batra, and Sehoon Ha. Hm3d-ovon: A dataset and benchmark for open-vocabulary object goal navigation. In *2024 IEEE/RSJ International Conference on Intelligent Robots and Systems (IROS)*, pages 5543–5550. IEEE, 2024b.

Zhuoyuan Yu, Yuxing Long, Zihan Yang, Chengyan Zeng, Hongwei Fan, Jiyao Zhang, and Hao Dong. Correctnav: Self-correction flywheel empowers vision-language-action navigation model. *arXiv preprint arXiv:2508.10416*, 2025.

Jiazhao Zhang, Kunyu Wang, Shaoan Wang, Minghan Li, Haoran Liu, Songlin Wei, Zhongyuan Wang, Zhizheng Zhang, and He Wang. Uni-navid: A video-based vision-language-action model for unifying embodied navigation tasks. *arXiv preprint arXiv:2412.06224*, 2024a.

Jiazhao Zhang, Kunyu Wang, Rongtao Xu, Gengze Zhou, Yicong Hong, Xiaomeng Fang, Qi Wu, Zhizheng Zhang, and He Wang. Navid: Video-based vlm plans the next step for vision-and-language navigation. *arXiv preprint arXiv:2402.15852*, 2024b.

Lingfeng Zhang, Yuecheng Liu, Zhanguang Zhang, Matin Aghaei, Yaochen Hu, Hongjian Gu, Mohammad Ali Alomrani, David Gamaliel Arcos Bravo, Raika Karimi, Atia Hamidizadeh, et al. Mem2ego: Empowering vision-language models with global-to-ego memory for long-horizon embodied navigation. *arXiv preprint arXiv:2502.14254*, 2025a.

Wenyao Zhang, Hongsi Liu, Zekun Qi, Yunnan Wang, Xinqiang Yu, Jiazhao Zhang, Runpei Dong, Jiawei He, Fan Lu, He Wang, et al. Dreamvla: a vision-language-action model dreamed with comprehensive world knowledge. *arXiv preprint arXiv:2507.04447*, 2025b.

Qingqing Zhao, Yao Lu, Moo Jin Kim, Zipeng Fu, Zhuoyang Zhang, Yecheng Wu, Zhaoshuo Li, Qianli Ma, Song Han, Chelsea Finn, et al. Cot-vla: Visual chain-of-thought reasoning for vision-language-action models. In *Proceedings of the Computer Vision and Pattern Recognition Conference*, pages 1702–1713, 2025.

Zhide Zhong, Haodong Yan, Junfeng Li, Xiangchen Liu, Xin Gong, Tianran Zhang, Wenxuan Song, Jiayi Chen, Xinhu Zheng, Hesheng Wang, et al. Flowvla: Visual chain of thought-based motion reasoning for vision-language-action models. *arXiv preprint arXiv:2508.18269*, 2025.

Siyuan Zhou, Yilun Du, Yuncong Yang, Lei Han, Peihao Chen, Dit-Yan Yeung, and Chuang Gan. Learning 3d persistent embodied world models. *arXiv preprint arXiv:2505.05495*, 2025.

Chuning Zhu, Raymond Yu, Siyuan Feng, Benjamin Burchfiel, Paarth Shah, and Abhishek Gupta. Unified world models: Coupling video and action diffusion for pretraining on large robotic datasets. *arXiv preprint arXiv:2504.02792*, 2025a.

Ziyu Zhu, Xilin Wang, Yixuan Li, Zhuofan Zhang, Xiaojian Ma, Yixin Chen, Baoxiong Jia, Wei Liang, Qian Yu, Zhidong Deng, et al. Move to understand a 3d scene: Bridging visual grounding and exploration for efficient and versatile embodied navigation. *arXiv preprint arXiv:2507.04047*, 2025b.

Brianna Zitkovich, Tianhe Yu, Sichun Xu, Peng Xu, Ted Xiao, Fei Xia, Jialin Wu, Paul Wohlhart, Stefan Welker, Ayzaan Wahid, et al. Rt-2: Vision-language-action models transfer web knowledge to robotic control. In *Conference on Robot Learning*, pages 2165–2183. PMLR, 2023.